Analysis of Cryogenic Propellant Liquefaction Rates in Cooled Constant-Wall-Temperature Tanks

Anson Koch[1], Ali Hedayat[2], Alok Majumdar[3], Andre Leclair[4],
NASA Marshall Space Flight Center, Huntsville, AL, 35812, United States

S. Mostafa Ghiaasiaan[5]
Georgia Institute of Technology, Atlanta, GA, United States

NASA has been focused on developing technology that would allow the production of cryogenic propellants on the Lunar and Martian surfaces. Utilizing Lunar/Martian resources, the produced gaseous propellants must first be liquefied and stored prior to use on the Moon or Mars ascent vehicle. Liquefaction of cryogenic propellants is a necessary technical development to enable NASA's future spaceflight goals. This paper presents an overview of a proposed model for a propellant liquefaction system, and the effect of tank wall temperature and the ullage pressure control band on cryogenic propellant liquefaction rates. The propellant system was assumed to be a receiver of a gas from an In-Situ Resource Utilization (ISRU) harvester and condensed the gas by cooling the tank walls. First, the heat transfer principles pertinent to condensation are summarized, followed by an overview of the model which performed the analysis, including a summary of the Fortran algorithm implementation. The sensitivity of the condensation rate relative to varying tank wall temperatures is also discussed.

I. Nomenclature

A_s	=	surface area
P	=	perimeter
$\overline{Nu}_L$	=	Nusselt number, averaged over characteristic length L
L	=	characteristic length
Re	=	Reynolds number
Pr	=	Prandtl number
Ra_L	=	Rayleigh number for characteristic length L
T_I	=	interphase temperature
T_{sat}	=	saturation temperature
T_{Fb}	=	wall temperature
T_G	=	vapor temperature
H_{FI}	=	interphase-wall heat transfer coefficient
H_{GI}	=	interphase-ullage heat transfer coefficient

[1] Aerospace Engineer, Propulsion Systems Department, NASA MSFC.
[2] Lead Aerospace Engineer, Propulsion Systems Department, NASA MSFC.
[3] Lead Aerospace Engineer, Propulsion Systems Department, NASA MSFC.
[4] Aerospace Engineer, Propulsion Systems Department, NASA MSFC.
[5] Professor, G.W. Woodruff School of Mechanical Engineering

h_{fg} = vaporization enthalpy
$_l$ = liquid region (subscript)
$_g$ = vapor/gas region (subscript)
$\dot{Q}_{BI}$ = Heat transfer rate between bulk gas and condensate film
$\dot{Q}_{IW}$ = Heat transfer rate between condensate film and tank wall
k = Thermal conductivity
σ = Surface tension
μ = Viscosity
δ = Film thickness
q'' = Alternate form for $\dot{Q}$
G = vapor/gas (subscript)
L = liquid (subscript)

II. Introduction

With the recent developments in ISRU technology, and the push to operate crewed space missions deeper into space beyond Low Earth Orbit (LEO), greater understanding of liquefaction processes is required to ensure mission success. Liquefaction is a combination of convection and condensation processes. Both processes must be modeled in detail, with special attention to the contributions each process makes to the mass and energy balance equations. This paper is based on modeling research into liquefaction processes, using detailed empirical heat transfer correlations. It also investigates the effects that different wall temperatures have on the entire liquefaction process. The heat transfer processes under analysis are modeled with widely-used empirical correlations. Better predictions on system performance will be of great benefit to mission designers, as they will not have to rely on intuition when making decisions regarding cryogenic liquefaction. This modeling effort focuses on integrating the relevant heat transfer mechanisms into a cohesive model, and has not yet been anchored to test data.

III. Modeling Approach

The modeling discussed herein assumes a cylindrical vessel with flat top and bottom. The vessel is oriented vertically with respect to gravity, and is assumed to be at Earth sea level gravity. This gravity was selected because many of the empirical correlations were developed at Earth gravity, and for ease of comparison to test data, which may be a future test case of this model. The choice of simple geometry allowed for the use of widely applied empirical correlations. The internal heat transfer processes are simulated over time with a constant time step, and various physical properties and variables are also tracked to aid in the model's insight. The ullage was assumed to be at a uniform thermodynamic state. The interfacial thermal resistance is negligible. The following section gives further detail into the methods used to model the heat transfer within each geometric domain: the vertical (cylindrical) section, the bottom plate, and the top plate.

Based on Nusselt's analytical approach for the condensation on a vertical plate and condensation models for the horizontal plates (top and bottom sections of tank), a computational model for the liquefaction process of gaseous propellant entering in a cryogenically refrigerated tank was developed. The model is incorporated into Generalized Fluid Flow Simulation Program (GFSSP), a Marshall Space Flight Center (MSFC) in-house developed software [1]. GFSSP is a fluid system analyzer program that has been used in a variety of propulsion systems analysis and design evaluation applications. Development of the proposed liquefaction model, its incorporation into GFSSP, and verification with available data will extend modeling capability and provide engineers with a more comprehensive tool that will allow them to design, perform trade studies, and optimize the entire ISRU system comprising various components (valves, flow passages, pumps, etc.) that may have an impact in reducing overall costs as well as increasing efficiencies of ISRU systems.

IV. OVERVIEW OF HEAT TRANSFER PROCESSES

A review of pertinent heat transfer processes and correlations is discussed in this section. The system in question assumes a cylindrical vessel in which condensation and convection occur. There is a source of gas flowing into this vessel to provide condensate mass. The flow rate is controlled to maintain gas pressure (ullage) at a predetermined pressure band, selected in consideration of typical propellant and tank structural requirements. The dominant heat transfer processes are convection and condensation. The effect of vapor condensation on the liquid-ullage surface is neglected for the purposes of this analysis. The primary focus is on the aforementioned heat transfer processes between the tank wall and the interior fluids (whether in liquid or gaseous phase).

The condensation model is based on the approach given by Ghiaasiaan [2]. The condensation rate is calculated by taking the following steps:

1. Heat Exchange between Interphase and wall, q''_{FI} : $q''_{FI} = H_{FI}(T_I - T_{Fb})$
2. Heat Exchange between Interphase and ullage, q''_{GI} : $q''_{GI} = H_{GI}(T_G - T_I)$
3. Condensation rate, m'': $m'' = (q''_{FI} - q''_{GI})/h_{fg}$

The above approach is applied to the cylindrical, top, and bottom segments of the cryogenically refrigerated tank. Each domain models the heat transfer according to their specific empirical relations. In each domain, the tank wall is assumed to be maintained at a constant temperature, which is also uniform throughout the tank material. The interface temperature T_I is assumed to be the same as the saturation temperature. The following subsections describe the modeling approach for each section of tank.

Vertical Cylindrical Section Model

Figure 1 shows the heat flow model for the vertical wall. Two heat flows are modeled: the heat moving from the bulk vapor into the condensate film, and the heat moving from the condensate film into the wall. The heat transfer coefficients were determined from Nusselt number correlations. For the vapor-to-condensate heat flow, the thermal conductivity of the gas was used in the Nusselt number equation to determine the heat transfer coefficient. For the condensate-wall heat flow, the liquid thermal conductivity was used.

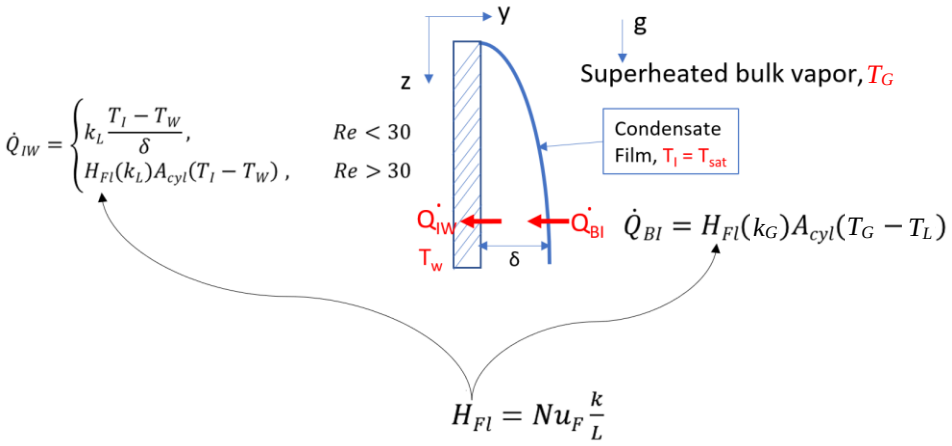

Figure 1: Heat Flow through Condensate Film on Vertical Wall [2]

Convection heat transfer between the ullage gas and the gas-liquid interphase over the vertical portion of the cylindrical wall is modeled by applying the empirical relation developed by Churchill and Chu [3]:

$$\overline{Nu}_L = \{0.825 + \frac{0.387 Ra_L^{\frac{1}{6}}}{\left[1+(0.492/Pr)^{\frac{9}{16}}\right]^{\frac{8}{27}}}\}^2 \qquad (1)$$

where all thermophysical properties represent the vapor phase.

For heat transfer between the vapor-liquid interphase and the wall (the liquid side thermal resistance) we use the following. For the condensate film, the Reynolds number is defined as:

$$\mathrm{Re}_F = 4\frac{\Gamma_F}{\mu_L}$$

where Γ_F is the condensate mass flow rate per unit width of the vertical surface. For $Re_{F,h_u} < 30$, where h_u represents the height of the vertical cylindrical surface covered by ullage, we simply assume a linear temperature distribution in the laminar liquid film and write $\bar{H}_F$ from Nusselt's analysis [2]. For $Re_{F,l} > 30$, we use the correlation of Chen et al. [6]:

$$\frac{\bar{H}_{\mathrm{F}}}{k_{\mathrm{L}}}\left(\frac{\nu_{\mathrm{L}}^2}{g}\right)^{1/3} = \left[\mathrm{Re}_{\mathrm{F},h_u}^{-0.44} + 5.82\times10^{-6}\,\mathrm{Re}_{\mathrm{F},h_u}^{0.8}\,\mathrm{Pr}_{\mathrm{L}}^{1/3}\right]^{1/2}$$

For simplicity, and due to uncertainties with respect to various aspects of the flow conditions, the effect of mass transfer on the convective heat transfer is not included.

It is assumed that the discrepancies between modeling a vertical flat plate and a vertical cylinder interior surface are negligible. This correlation is applicable whether the wall surface is in contact with liquid or vapor. The characteristic length L changes as a function of the liquid height, and this correlation is applied in both the liquid and vapor regions of the vertical wall.

Top of Tank Model

For the top of the tank, as shown in Figure 2, Rohsenow [4] recommended an empirical Nusselt number correlation as a function of the Rayleigh number for the liquid side heat transfer coefficient:

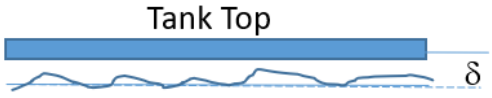

Figure 2: Condensation Film on Tank Top Surface

$$Nu_m = \begin{cases} 0.69Ra^{0.20}, & 10e6 < Ra < 10^8 \\ 0.81Ra^{0.193}, & 10e8 < Ra < 10^{10} \end{cases} \qquad (4)$$

The heat transfer coefficient h_m for the top surface is then calculated from the following Nusselt number equation, modified to account for the phase boundary [4]:

$$Nu_m = \frac{h_m}{k_l}\left(\frac{\sigma}{g(\rho_l - \rho_g)}\right)^{1/2} \qquad (5)$$

The Rayleigh number used in equation 4 is found from the following relationship [4]:

$$Ra = \frac{g\rho_l(\rho_l-\rho_g)h_{fg}}{\mu_l\Delta T k_l}\left(\frac{\sigma}{g(\rho_l-\rho_g)}\right)^{3/2} \qquad (6)$$

Where h_{fg} refers to the latent heat of vaporization, σ refers to the surface tension, and the subscripts l and g refer to the liquid and gas phases, respectively. Together, equations 4, 5, and 6 yield a heat transfer coefficient describing the heat flow between the condensate film and the tank material.

For the the vapor side heat transfer coefficient (heat transfer between ullage and the vapor-condensate interphase on the top surface of the tank), the Nusselt number can be found from the following correlation of McAdams [7] (see Incropera and DeWitt [5]):

$$\overline{Nu_L} = 0.27 Ra_L^{1/4} \qquad (10^5 \lesssim Ra_L \lesssim 10^{10}) \qquad (7)$$

This Nusselt number then gives the heat transfer coefficient for the heat flow from the vapor to the condensate film. The film thickness on the top plate was assumed to be 0.1 in. For the Rayleigh and Nusselt numbers the characteristic length factor L is the diameter of the top plate.

Bottom of Tank Model

For the bottom of the tank, as shown in Figure 3, the heat transfer can be modeled as conduction across the collected condensed liquid (no convection occurs because the bottom surface is colder than fluid above). The height of this liquid grows as more mass is condensed out of the vapor. The tank bottom conduction can be modeled by the following correlation [4]:

$$q_L'' = \frac{k_L}{\delta}(T_L - T_w)$$

Where it is assumed that the T_L interface temperature is the saturation temperature and T_w is the tank wall temperature. In this case, the δ is simply the condensed liquid height.

A similar relationship is applicable for modeling conduction through the ullage region.

$$q_G'' = \frac{k_G}{h_u}(T_G - T_L)$$

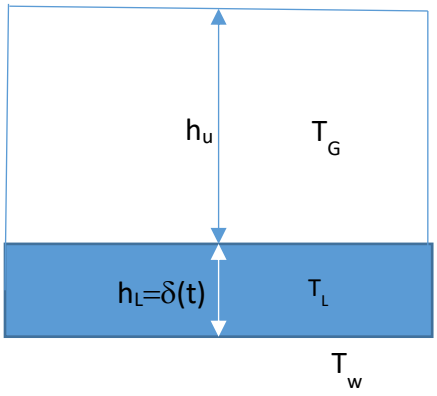

Figure 3: Condensation Film on Tank Bottom Surface

V. Generic Model Results

Initial development of this model focused on a generic case, which was selected using common parameters in cryogenic systems. The main purpose of this generic case was to simplify model development, prior to performing any parametric analysis activities. The generic case assumed a small tank 1 foot in diameter and 1 foot in height, with the tank walls held to a constant temperature of $-330°F$. Nitrogen was selected as the source gas, with the tank held at 37 ± 1 psi. GFSSP was configured to operate a valve using a simple bang-bang algorithm to control the ullage pressure within this pressure band. Figure 4 shows the condensate mass increasing over the simulation time. Figure 5 shows that the model correctly handles changes in the ullage and liquid volumes and conserves it correctly.

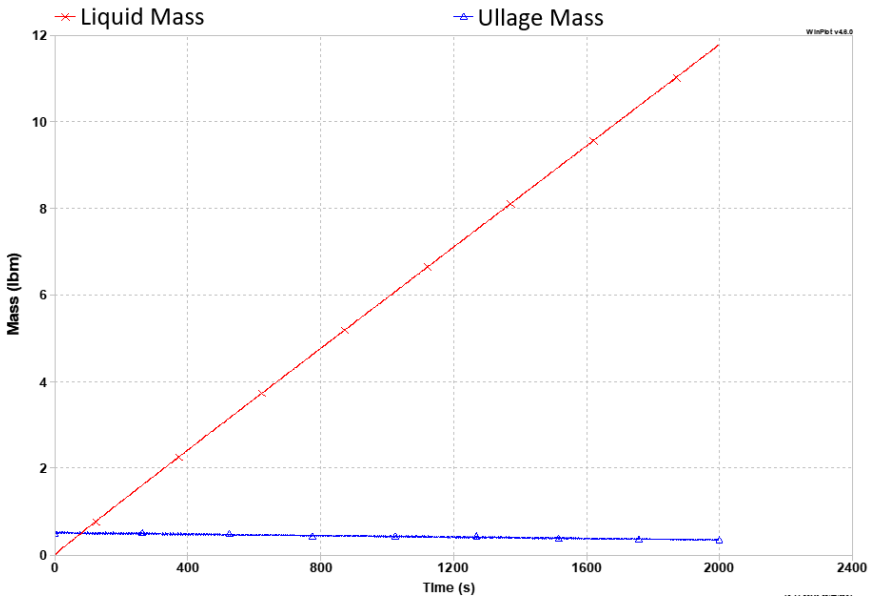

Figure 4: Mass of Liquid and Ullage for Generic Case

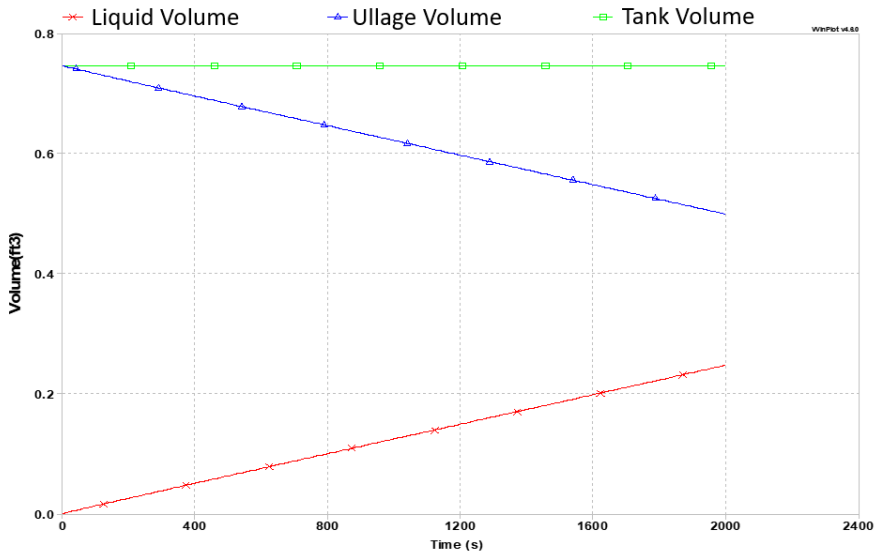

Figure 5: Volume Histories for Generic Case

VI. Analyzing Varying Tank Wall Temperatures

This work involves exploring the effect that different wall temperatures have on the liquefaction rate. The goal is to obtain reasonable projections for the operating profile of a liquefaction system, which can provide initial estimates for valve cycle fatigue requirements, for example. shows the total condensed mass as a function of time for different wall temperatures. The stated subcooling amount is relative to the ullage gas saturation point. As can be expected, colder tanks will condense a greater amount of liquid. This model can predict the quantitative difference in condensed mass due to different temperatures, which is a valuable relationship to consider for mission planning purposes.

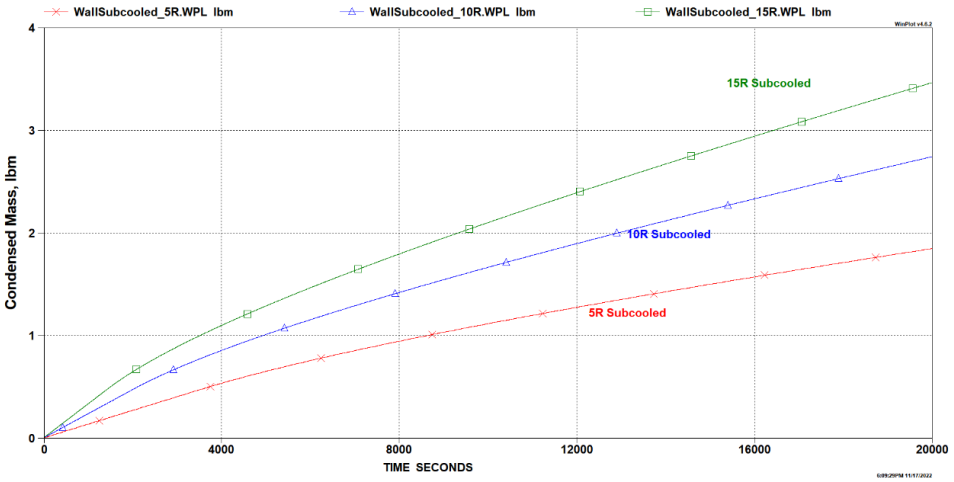

Figure 6: Condensed Mass History for 5, 10, and 15R Subcooled Tank Walls

VII. Analyzing Alternative Pressure Control Bands

To support various mission architectures, this model also can examine how the liquefaction system performs for different tank pressure control bands. Early mission trade studies may analyze a range of different control pressures, so it is important for this model to account for how the liquefaction performance is affected by this parameter. The baseline case for this model assumed a pressure of 37 +/- 1 psia. The other comparison cases were run at 27 +/- 1 psia, and 17+/- 1 psia. These were selected as being representative of typical propellant tank pressures that one might expect to see in a trade study. Figure 7 shows the condensate mass history for these three cases. Many of the inputs to the heat transfer relations are functions of ullage gas density, which is also dependent on ullage pressure.

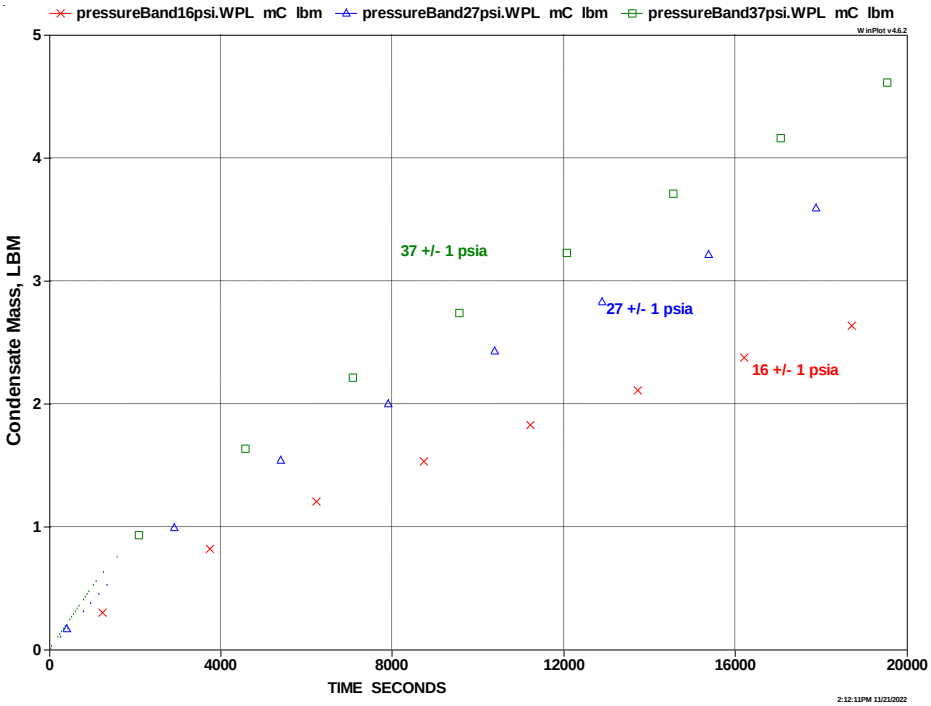

Figure 7: Varying Ullage Pressure Control Band

VIII. Conclusion and Future Work

The modeling developments from this work have been largely influential on a similar GFSSP model that MSFC developed to account for the effect that ellipsoidal or hemispherical tank endcaps have on condensation rates and heat transfer rates. The parametric analysis shown here will form the basis for detailed parametric analyses with this more detailed model.

Once the parametric analysis space is defined for the more detailed model, it will then be anchored against available test data. After anchoring the models to this data, they will be ready for use as analysis tools for planning space missions involving ISRU or cryogenic liquefaction as part of their operational concept.

References

1. Majumdar, Alok and Leclair, Andre. GFSSP, "Generalized Fluid System Simulation Program," Ver. 6.0, User Manual, March 2016, NASA/TP-2016-218218.
2. Ghiaasiaan S. M., *Two-Phase Flow, Boiling, and Condensation*, 2nd ed., Cambridge University Press, 2017.
3. Churchill, S. W., and H. H. S. Chu, *Int. J. Heat Mass Transfer*, 18, 1323, 1975.
4. Rohsenow, W.M., Hartnett, J.P., Cho, Y.I., *Handbook of Heat Transfer*, 3rd ed., McGraw-Hill, 1998.
5. Incropera, F., DeWitt, D. P., Bergman, T.L., Lavine, A.S., *Fundamentals of Heat and Mass Transfer*, 6th ed., Wiley, 2006.
6. Chen, S. L., Gerner, F. M., and Tien, C. L. (1987). General film condensation correlations. *Exp. Heat Transfer*, 1, 93–107.
7. McAdams, W. H. (1954). *Heat Transmission*, 3rd ed., McGraw-Hill, New York.